



Digitally controlled multiplexed silicon photonics phase shifter using heaters with integrated diodes

ANTONIO RIBEIRO^{1,2,*} AND WIM BOGAERTS^{1,2}

¹Photonics Research Group, Ghent University-IMEC, Ghent, Belgium

²Center of Nano and Biophotonics, Ghent, Belgium

*Antonio.Ribeiro@UGent.be

Abstract: We present a silicon side heater with integrated diode to provide multiplexed control of different elements in a photonic circuit based on the polarity of the driving signal. The diode introduces an asymmetric electrical response where the heater is only active under forward bias. This can be used to address multiple heaters through the same electrical electrical contacts. We demonstrate push-pull operation on a Mach-Zehnder interferometer with heaters in both arms, as well as time-multiplexed operation of multiple heaters by modulating the driving signal. We extend this work by demonstrating how *pulse width modulation* (PWM) and duobinary-PWM can be used to improve the linearity of the response of the phase shifters.

© 2017 Optical Society of America under the terms of the [OSA Open Access Publishing Agreement](#)

OCIS codes: (130.3120) Integrated optics devices; (130.4815) Optical switching devices; (130.4110) Modulators.

References and links

1. M. R. Watts, J. Sun, C. DeRose, D. C. Trotter, R. W. Young, and G. N. Nielson, "Adiabatic thermo-optic Mach-Zehnder switch," *Opt. Lett.* **38**, 733–735 (2013).
2. G. T. Reed, G. Z. Mashanovich, F. Y. Gardes, M. Nedeljkovic, Y. Hu, D. J. Thomson, K. Li, P. R. Wilson, S. Chen, S. S. Hsu, "Recent breakthroughs in carrier depletion based silicon optical modulators," *Nanophotonics* **3**(4-5), 229–245 (2013).
3. Y. Maegami, G. Cong, M. Ohno, M. Okano, and K. Yamada, "Strip-loaded waveguide-based optical phase shifter for high-efficiency silicon optical modulators," *Photon. Res.* **4**, 222–226 (2016).
4. Y. Yang, Q. Fang, M. Yu, X. Tu, R. Rusli, and G. Lo, "High-efficiency Si optical modulator using Cu travelling-wave electrode," *Opt. Express* **22**, 29978–29985 (2014).
5. J. Komma, C. Schwarz, G. Hofmann, D. Heinert, and R. Nawrodt, "Thermo-optic coefficient of silicon at 1550 nm and cryogenic temperatures," *Appl. Phys. Lett.* **101**(4), 041905 (2012).
6. A. Masood, M. Pantouvaki, G. Lepage, P. Verheyen, J. Van Campenhout, P. Absil, D. Van Thourhout, W. Bogaerts, "Comparison of heater architectures for thermal control of silicon photonic circuits," *Group IV Photonics*, South Korea (2013), p.ThC2.
7. A. Masood, M. Pantouvaki, D. Goossens, G. Lepage, P. Verheyen, J. Van Campenhout, P. Absil, D. Van Thourhout, W. Bogaerts, Fabrication and "Characterization of CMOS-compatible integrated tungsten heaters for thermo-optic tuning in silicon photonics devices," *Opt. Mater. Express* **4**(7), 1383–1388 (2014).
8. D. Schall, M. Mohsin, A. Sagade, M. Otto, B. Chmielak, S. Suckow, A. Giesecke, D. Neumaier, and H. Kurz, "Infrared transparent graphene heater for silicon photonic integrated circuits," *Opt. Express* **24**, 7871–7878 (2016).
9. B. Lee, M. Zhang, F. Barbosa, S. Miller, A. Mohanty, R. St-Gelais, and M. Lipson, "On-chip thermo-optic tuning of suspended microresonators," *Opt. Express* **25**, 12109–12120 (2017).
10. A. Rosa, A. Gutierrez, A. Brimont, A. Griol, and P. Sanchis, "High performance silicon 2x2 optical switch based on a thermo-optically tunable multimode interference coupler and efficient electrodes," *Opt. Express* **24**, 191–198 (2016).
11. L. Yu, Y. Yin, Y. Shi, D. Dai, and S. He, "Thermally tunable silicon photonic microdisk resonator with transparent graphene nanoheaters," *Optica* **3**, 159–166 (2016).
12. P. P. Absil, P. Verheyen, P. D. Heyn, M. Pantouvaki, G. Lepage, J. D. Coster, and J. V. Campenhout, "Silicon photonics integrated circuits: a manufacturing platform for high density, low power optical i/o's," *Opt. Express* **23**, 9369–9378 (2015).
13. W. Bogaerts, M. Fiers, M. Sivilotti, and P. Dumon, "The ipkiss photonic design framework," *Optical Fiber Communication Conference*, (Optical Society of America, 2016), p. W1E.1.

1. Introduction

Heaters are an attractive solution for phase shifting in silicon photonics due to their simplicity of implementation and compactness, compared to alternatives such as free-carrier modulators [1–4]. The high thermo-optic coefficient of silicon ($1.8 \times 10^{-4} K^{-1}$) makes devices susceptible to temperature variations [5], and allows efficient tuning of wavelength filters and spectrum shifting [6–11]. Although compact, heaters often require large contact pads to connect to external electronics for driving. Such pads can occupy a considerable area in a photonics integrated circuit (PIC) and become a limiting factor for its scalability and packing density. We present a method to save space by multiplexing the use of the pads, driving multiple heaters independently with the same set of pads.

Resistive heaters can be implemented using multiple approaches. A typical side heater consists of a doped silicon strip placed close to the target waveguide, and is controlled as an electric resistor. The resistivity of the heater is determined by its electrical properties (both inherent from the silicon and obtained from its dopants) and its geometry.

Because such side heaters are pure resistive elements, the heaters have a symmetric response to the driving voltage. Inverting the polarity of the driving signal will have no effect whatsoever on the response of the phase shifter. To break this symmetry we introduced a diode in series with the heater element, making it work only in forward biased and acting as an open electrical circuit when reverse biased. The circuit is represented in Fig. 1 (a).

If we place two such diode-loaded heaters in parallel and connect the cathode of one heater to the anode of the other, and vice versa [Fig. 2(c)], we can use a single pair of contact pads to drive either one heater or the other, depending on the polarity of the applied voltage. This scheme can be further explored by driving the device with a variable signal over time instead of a direct current (DC) voltage. A variable signal that contains both a positive and a negative cycle, each independently adjustable, can be used to time-multiplex the control to the heaters.

Another characteristic of conventional heaters is that the induced phase shift grows quadratic with the applied voltage (as the phase shift is proportional to the temperature change of the silicon, which is proportional to the electrical power dissipated by the heater). This, together with the non-linearity of an imperfectly fabricated heater and the temperature dependent electrical properties of silicon, results in a non-linear phase-shift/voltage response of the device, which can increase the complexity of feedback systems used to drive the thermo-optic phase shifter. We present an alternative to obtain a linear response from the phase shifters by digitally driving them using a *pulse width modulation* (PWM) signal instead of a DC signal. This approach delivers a much more linear phase shift response in function of the driving parameter, in this case the duty cycle of the PWM.

2. Design and fabrication

To demonstrate the diode-loaded heater we implemented it using a doped silicon strip heater. On a typical side heater, the silicon strip is doped with either *P-type* or *N-type* dopants to increase its conductivity. In our design we doped the main body of the heater using *N-type* dopants, and near one of the electrical contacts we used a *P-type* dopant, creating a *PN* junction inside the heater. This approach converts the standard heater to a diode in series with a high resistivity strip. The total length of our heater is $50\mu m$, where $8\mu m$ is used for the *P-type* doped region. The value of $8\mu m$ was chosen to minimize the size of the *P-type* doped section, as it has lower conductivity when compared with the *N-type* doped silicon. The width of the heater is $1.2\mu m$. The heaters are placed close to the target waveguide [Fig. 1(a)], keeping a gap of $0.75\mu m$ between the heater and the waveguide. The gap was chosen to be close enough to increase the power efficiency of the heater and yet avoid the optical mode to leak from the waveguide to the heater. The heater and the waveguide have a different width to minimize coupling due to phase matching.

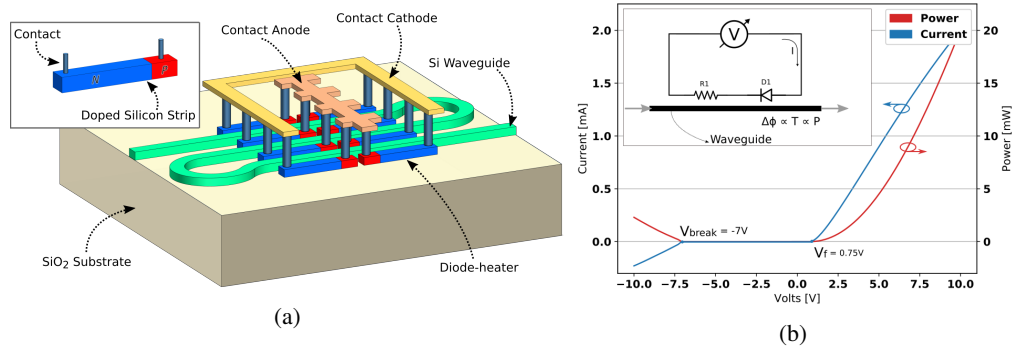


Fig. 1. (a) The diode heater is implemented as a side heater using a strip waveguide (insert). Multiple heaters can be placed in parallel to increase the power output, and the waveguide can be routed to surround the heaters, increasing the power efficiency of the phase shifter. (b) The equivalent electric circuit (insert) and the I-V curve of a measured device shows a clear diode behaviour, with negligible current flow (and power dissipation) for reverse bias up to $-7V$.

We implemented the device in imec's ISIPP25G+ silicon photonics platform through the Europractice MPW service using established building blocks from the supplied process design kit (PDK) [12]. The circuit was designed using the IPKISS toolset from Luceda Photonics [13] and the circuit was simulated using the Caphe circuit simulator, which is integrated with IPKISS. The silicon waveguides are $450nm$ wide and $220nm$ thick, with an additional $2\mu m$ of oxide as a top cladding. The platform also offers two layers of metal for electrical routing (copper) and aluminium bondpads for external interfacing.

To demonstrate the phase shifters we placed them in two different designs: in an asymmetric *Mach-Zehnder Interferometer* (MZI) [Fig. 2(b)] in a pair of ring resonators with slightly different resonances [Fig. 2(a)]. The MZI is implemented using standard 2×2 multimode interferometers (MMI) as splitter/combiner and strip waveguides as its arms. The MZI arm length is $763\mu m$ and the extra length in one of the arms is $\Delta L = 62\mu m$, giving an *free spectral range* (FSR) of $9nm$. The calculated value of the FSR was confirmed in the circuit simulation. To reduce the total footprint of the MZI the arms were folded [Fig. 1(a)]. This also allowed a more compact placement of the heaters, which helps to increase the power efficiency of the device. Rather than a single large heater, we applied 8 smaller heaters on each arm (to reduce total electrical resistance, connected in parallel with the same polarity), which allows us to deliver sufficient electrical power at lower voltages. Fig. 3 shows the fabricated MZI.

For the ring resonators we designed two rings with slightly different length which let us observe two different resonances in the spectrum. For the larger ring the total length is $L = 107.4\mu m$ while the smaller has a roundtrip length of $L = 101.4\mu m$. For both rings the circular area was constructed with the same radius ($5\mu m$) and the same gap for the directional couplers ($0.2\mu m$). The power coupling coefficient of the directional coupler was extracted from a 3D FDTD simulation, with a value of $\kappa = 0.02$.

The optical input and output of the circuits are done via vertical coupling using grating couplers while the electric interface is established using contact probes via aluminium bondpads.

3. Electrical and optical characterization

We characterized the fabricated diodes by extracting its I-V curve. We used a variable voltage source to drive the heater within a voltage range of $-10.0V$ to $+10.0V$, while recording the current through the device. The I-V curve of the fabricated devices [Fig. 1(b)] shows a clear

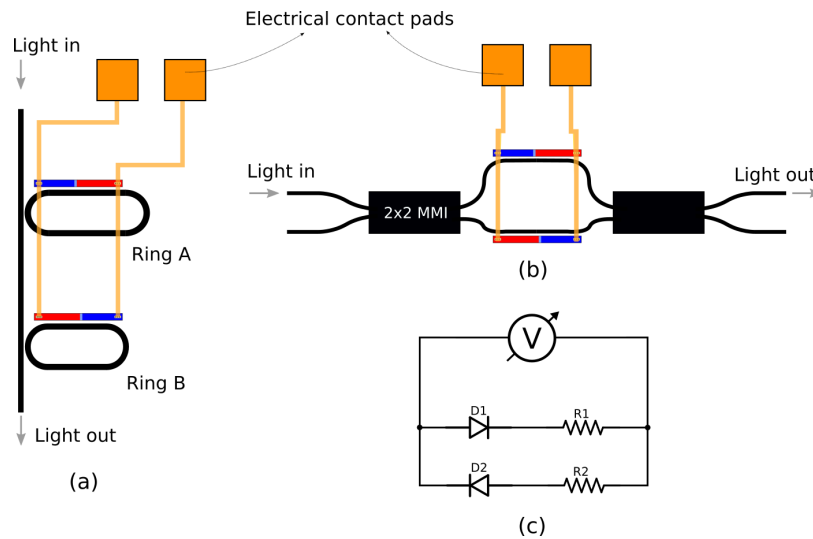


Fig. 2. (a) Schematic of the ring resonators circuit, (b) schematic of the MZI with diode heaters in a push-pull configuration, and (c) the electric circuit equivalent. For a given polarity either $D1$ or $D2$ will be conducting.

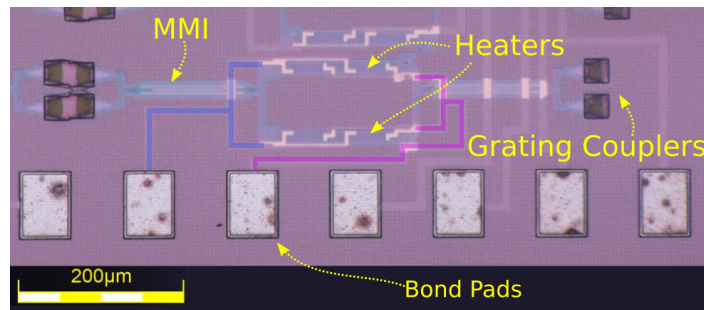


Fig. 3. Microscope image of the fabricated MZI using diode heaters on both arms to operate in push-pull configuration.

diode behavior, with negligible current flow in reverse bias, before the breakdown point. All measured diodes yielded similar values for the conduction threshold voltage (around $0.75V$) while the reverse breakdown voltages stayed at around $-7V$ for all the cases. From this values, we assume that it is safe to operate the heaters in the $\pm 7V$ forward bias range without inducing any phase shift in the heaters connected to the same pads, but with opposite polarity.

The measured resistance at $5V$ was $5.3k\Omega$ and the electrical power delivered at $7V$ was $9.6mW$ per heater. To achieve higher power output without compromising the operational range of $\pm 7V$ we can drive multiple heaters in parallel. For the MZI circuit the eight heaters placed on each arm could deliver up to $76.8mW$ at $7V$. The ring resonator circuit is equipped with two heaters per ring, allowing us to apply up to $19.2mW$ at $7V$.

For the optical characterization of the circuit we measured the insertion loss and the extinction ratio of the MZI and the ring resonators. The measured insertion loss for the MZI was $-1.6dB$ while for the rings we obtained the best result of $-1.9dB$. The MZI could deliver an extinction ratio of up to $40dB$ while for the rings circuit we obtained $-20dB$ for the ring A and $14dB$ for the ring B . The observed FSR for the MZI agrees with calculated and simulated values of $9nm$ [Fig.

4(a)]. All the measurements were performed with the samples placed on a temperature controller device at constant 25°C .

To extract the heater efficiency we operated the MZI phase shifters while monitoring the spectrum shift of the device [Fig. 4(a)] and recorded the voltage and current values necessary to obtain a πrad phase shift (half FSR in the spectrum profile). From the obtained values we report a πrad phase shift at 20.9mW , which is a result compatible with the reported values for this technology [6].

4. Applications

We illustrate the possibilities of the device showing two applications where the number of pads necessary to operate the circuit is reduced by exploiting the asymmetry of the diode-loaded heater. In the first case we show an MZI filter in push-pull configuration, where at a given time either one of its two phase shifters is operating. The selection of the actuating heater is given by the polarity of the driving signal. For a second application we demonstrate how the use of a modulated signal can provide simultaneous control of two ring resonators in an independent fashion, yet using a single pair of contact pads.

4.1. Red-Blue shifting of MZIs filters

To demonstrate the diode heaters we implemented a MZI circuit operating it in push-pull configuration. A typical MZI operating in push-pull configuration needs at least three contact pads to operate, using a common-ground (one pad for the ground level and one pad for each heater). We designed our MZI circuit with diode heaters in both arms and routed the electric connections in such way that, depending on the bias of the driving signal, either one arm or the other will be addressed [Fig. 2 (b)]. The mutually exclusive operation is guaranteed within the $\pm 7\text{V}$ operation range, since no current was observed in reverse bias in this range [Fig. 1(b)]. This scheme allowed us to operate the circuit in push-pull configuration with only one pair of pads.

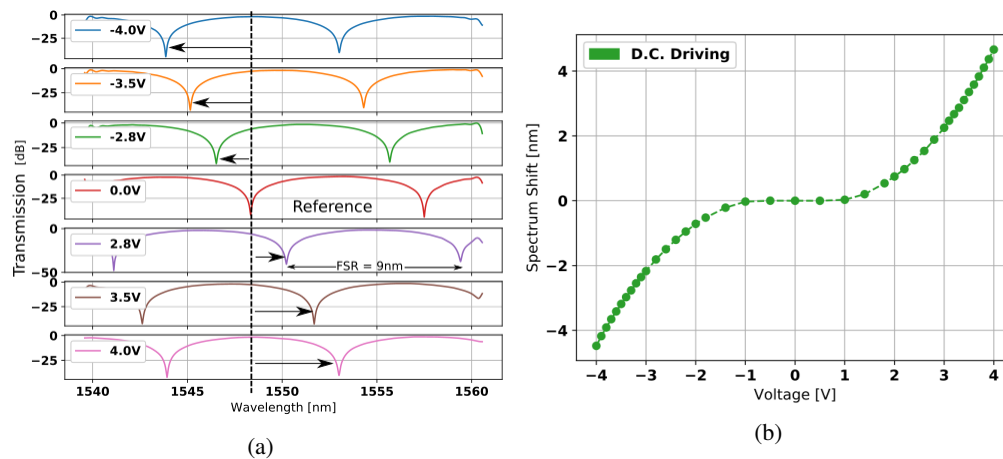


Fig. 4. (a) The response of the measured MZI for different driving DC voltages and (b) the correlation between the applied voltage and the obtained spectrum shift (in nm).

In Fig. 4(a) we show the spectrum profile of the MZI in inactive state (center row, in red). Using this as a reference, we can show that driving the heaters with a DC signal will induce a shift in the spectral response of the MZI, and the direction of the shift depends on the polarity of the DC signal. For the first three rows we can see a blue-shift of the spectrum and in the bottom three rows, when we apply a signal with an inverted polarity, we observe a red-shift of the

spectrum. In Fig. 4(b), we can see the measured spectrum shift (in nm) induced by the heaters as a function of the driving voltage. It is clear from this results that the circuit has two operating regimes, one for blue shift and other for red shift, depending on the bias of the driving signal. We can also observe a region between $-1V$ and $+1V$ where we have almost no response from the heaters, because the bias is below the threshold voltage of the diode ($0.75V$). Outside this region the dissipated power grows quadratically with the applied voltage.

4.2. DC vs PWM driving

Driving a heater with a DC signal, although the most straightforward approach, comes with some drawbacks. The phase shift response of the heater grows proportional to the silicon temperature, which is proportional to the dissipated power. A perfect heater has a power-vs-voltage response that grows quadratically with the increase of the applied voltage. For a real heater the non-linear response of the heater adds extra complexity to this behavior. For a heater with an integrated diode we also have to take in account the region where, although forward biased, the diode is not conductive because it didn't reach the threshold voltage. The quadratic response of the heater and the non-conducting region ($V < V_{threshold}$) can be seen in Fig. 4(b).

As a solution for the linearity response of the phase shifter we propose the use of a digital PWM signal to drive the heaters. In a PWM signal with fixed amplitude the delivered power, integrated over time, is proportional to the duty cycle of the signal. That means that a linear increase in the duty cycle of the PWM signal will result in an equally linear phase shift induced by the heaters. In Fig. 5(a) we show a change in the spectrum profile of the MZI in function of the duty cycle of the PWM driving signal. A signal with a negative duty cycle indicates a PWM signal with negative bias. The spectrum shift in function of the PWM duty cycle can be compared with the DC driving technique in Fig. 5(b). From this comparison it is very clear that the phase shifter has a much more linear response for a PWM signal with fixed amplitude when compared to a DC driving signal. Such technique can be used to simplify the drivers for thermo-optic phase shifters (once a fixed voltage source is used, instead of a variable one) and to improve its control due to the quasi-linear response of the device.

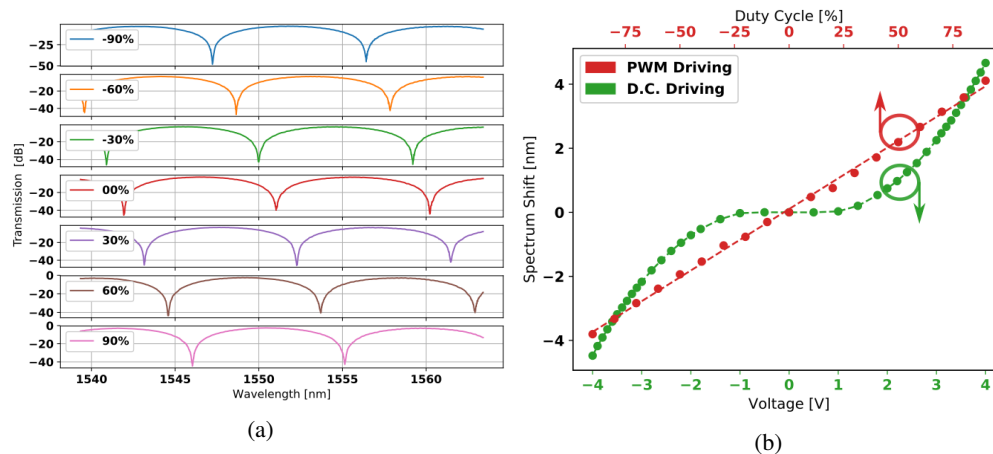


Fig. 5. (a) Spectrum shift as function of duty cycle of the PWM driving signal and (b) a comparison between the spectrum shift in function of a DC driving signal and a PWM signal. The points where the duty cycle value is negative indicates that the polarity of the PWM signal is negative. For the PWM measurement we applied a signal with a frequency $f = 2MHz$ with an amplitude of $5V$.

We operated the heaters with a $2MHz$ PWM signal with a fixed amplitude of $5V$. This is

sufficient to maintain a stable phase shift as it is much faster than the thermal time constant of the heater-waveguide system. We performed multiple instances of the measurement to ensure the repeatability of the system. We did not record any fluctuation in the spectrum shift for a given driving signal that is relevant to report. The characterization of the minimum driving frequency of the PWM signal is discussed in section 5.

4.3. Simultaneous control using PWM signal with two bias

In Fig. 6 we show the spectral response of the two-ring circuit [Fig. 2(a)] for different driving signals, with different bias. As the circuit was designed following a scheme similar to the one explored by the MZI in push-pull configuration, only one ring will respond to a positive driving signal, and the other to the negative signal. Of course, in such a circuit, it is important to address both heaters in an independent fashion and at the same time, to provide a real multiplexed use of the electrical pads.

To obtain such result we used a time-multiplex signal that contains both a positive cycle and a negative one, allowing to address both heaters simultaneously. This signal, a *duobinary PWM*, contains two alternating PWM pulses, one with positive polarity followed by one with negative polarity. The duty cycle of both pulses can be controlled independently, which allows independent control of the heaters. Additionally, as the phase shift induced by a PWM signal is linear in function of its duty cycle, the spectrum shift induced in the ring resonator also responds linearly to the driving signal. In Fig. 7, bottom rows, we can see a representation of the duobinary PWM signal used to control the heaters.

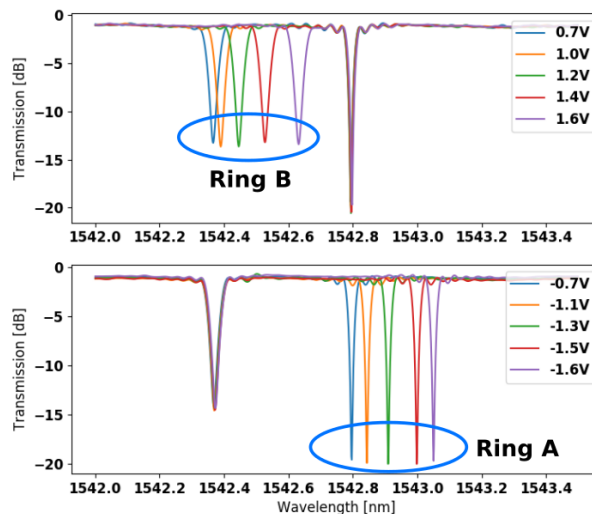


Fig. 6. The spectral response of the ring resonator circuit as a function of the applied voltage at the contact pads. Depending on the polarity of the driving signal either *Ring A* or *Ring B* will respond to the stimulus.

To demonstrate the individual control of the two heaters in the ring circuit we applied several combinations of the duobinary signal while measured the shift in spectrum dips from the rings. In Fig. 7(a) we show the correlation between the duty cycle values of both the positive and the negative part of the duobinary signal (rows 1 and 3) and the measured phase shift induced on each ring resonator (rows 2 and 4), as well as the driving signal (bottom). From this we can visualize that a change in the duty cycle of the positive part of the signal affects only the *Ring B* while a change in the duty cycle of the negative part of the signal will result in a response of the *Ring A*

only. This demonstrates that we can use one pair of pads to control two heaters at the same time, in an independent fashion.

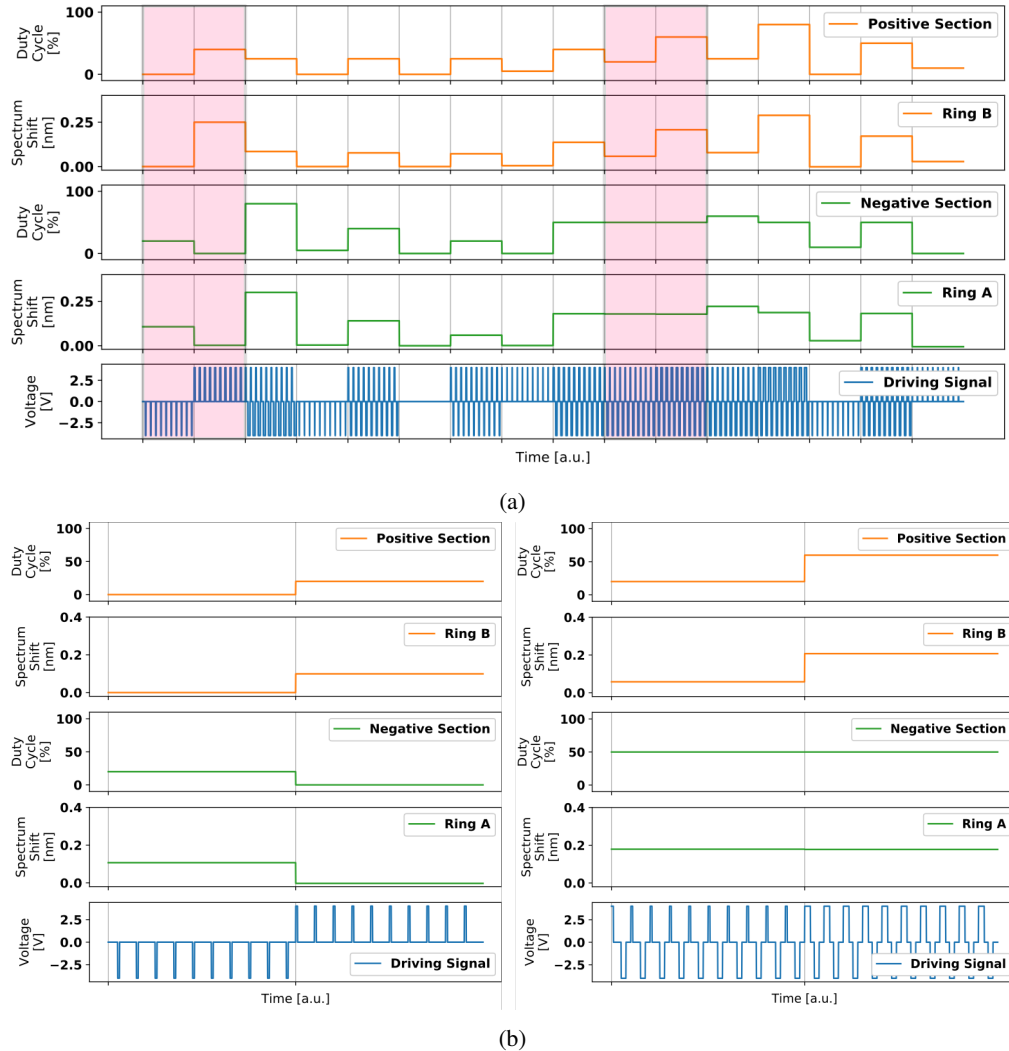


Fig. 7. (a) Correspondence between the duty-cycle values of the duobinary PWM driving signal (rows 1 and 3) and the measured spectrum shift for the resonances of the two rings (rows 2 and 4). The bottom row shows the respective duobinary PWM signal. (b) Zoomed-in traces of transitions showing the change in the duobinary PWM signal.

Although the electrical cross-talk between the diodes with opposite polarity can be considered negligible once the operation values are far from the breakthrough voltage ($-7V$), a thermal cross-talk between the devices could be observed. Such effect can be minimized by placing the elements sufficiently far apart to decrease the thermal cross-talk.

As we are time-multiplexing the use of the pads we have to take in account that, in the best case, only 50% of the total signal period can be used to drive one heater (as the remaining 50% should remain available to be used by the second heater, with a different signal polarity). As a consequence this reduces by half the maximum achievable phase shift, compared to a

non-time-multiplexed heater. To compensate for this we chose to over-dimension our phase shifter by adding multiple heaters in parallel, delivering high output power at lower voltage (or lower duty cycles) that remains below the breakthrough limit of $7V$.

For the demonstrated multiplexed operation of the circuit we used a duobinary signal with a fixed peak voltage of $\pm 3V$ and a frequency of $5MHz$.

5. Frequency domain analyses of the phase shifter response

The use of digital PWM signal to drive the phase shifters only is possible due to the very high time-constant of such devices. The resulting phase shift is proportional to the temperature of the silicon, so if we are able to deliver a digital signal that changes much faster than the thermal reaction time of the circuit, the resulting heat delivered by the heater to the waveguide will be averaged over the driving period proportional to the duty cycle of the driving signal.

A simplified thermal resistor-capacitor (RC) model of the device can be seen in Fig. 8(a). In our model we assume that all the delivered heat will be drained to the silicon substrate (our thermal ground level). The heat delivered by the heater is conducted to both the waveguide (via R_s) and to the substrate (via R_{he}). The heat from the waveguide flows to the substrate via R_{wg} . Both the heater and the waveguide contain a capacitor-equivalent element (C_{he} and C_{wg}) that models the stored heat in each element. The RC constant given by the capacitor and the resistor dictates the heat-up and cool-down time of the system.

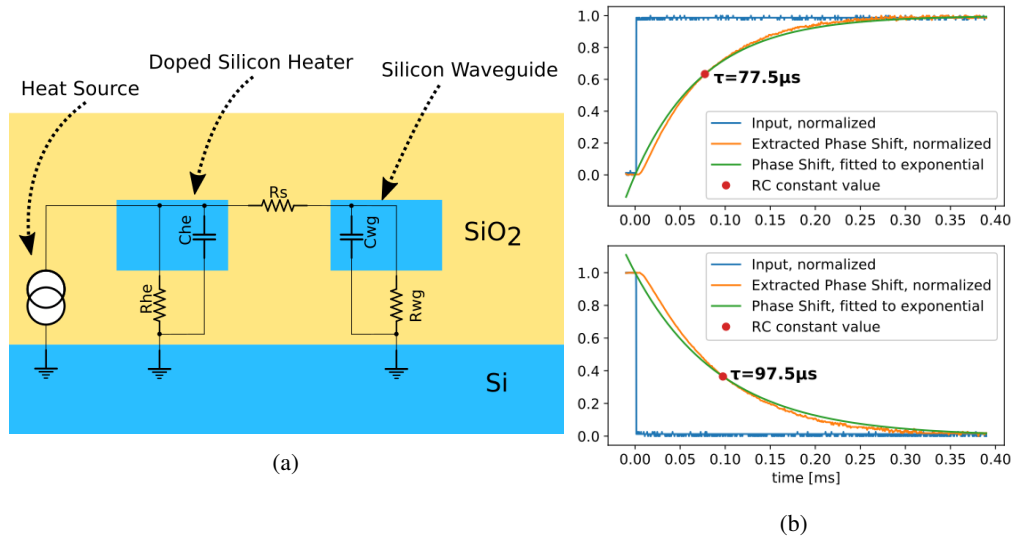


Fig. 8. The thermal RC model of the phase shifter(a) is used to determine the frequency domain response of the phase shifter. From the transient response of the circuit(b) it is possible to extract its RC constant (τ) and feed it back to the RC model. The obtained values for the RC constants were $\tau_{charging} = 77.5\mu s$ and $\tau_{discharging} = 97.5\mu s$.

To extract the RC time constant of the phase shifter we used the MZI circuit operated as a switch. We applied an electric signal to switch the MZI from a bar to a cross configuration and measured its transient response. The result is seen in Fig. 8(b), where we plot the phase change over time for a step variation in the driving signal. We observed slightly different RC constants for the heat-up and cool-down phases ($\tau_{charging} = 77.5\mu s$ and $\tau_{discharging} = 97.5\mu s$). As we want to determine the minimum signal frequency needed to drive the circuit without observing phase shift fluctuations across the time, we assume that the RC constant of the circuit is the result

for the worst-case scenario, so $RC = \tau_{charging} = 77.5\mu s$.

With the obtained value we recreated the RC model in a SPICE circuit simulation. As a first approximation we assume $R_{he} = R_s = R_{wg}$ and $C_{he} = C_{wg}$. The resulting frequency response of the circuit is visualized in Fig. 9(a). At 100KHz we can observe a signal intensity attenuation close to 30dB while at 1MHz the figure is close to 40dB . The result agrees with the measurements shown in Fig. 9(b), where we show the phase change over time for driving signal with different frequencies. We clearly notice that the phase shift over time is not constant for low frequencies, especially in the top row, at 10KHz . In the bottom row, for a driving frequency of 500KHz , we can only notice the average induced phase shift without fluctuation over time. The result indicates that it is safe to operate the circuit using a PWM signal which period is smaller than $2\mu s$ ($f > 500\text{KHz}$).

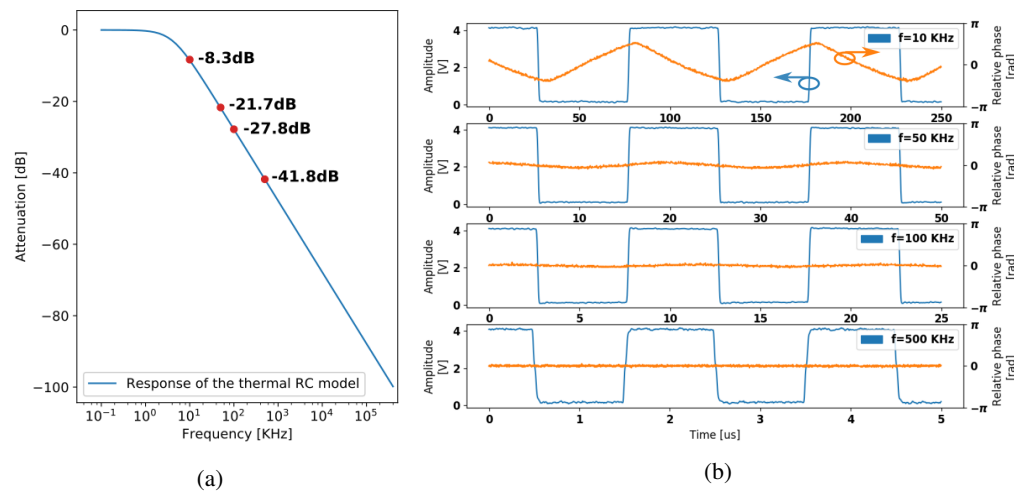


Fig. 9. (a) The measured RC constant is used to feed the RC model and, with that, obtain the frequency domain response of the circuit. (b) The measured relative phase shift fluctuation for different frequencies of the PWM signal shows a constant phase response for the signal frequency $f = 500\text{KHz}$. The expected attenuation for the frequencies plotted in (b) are marked in the diagram in (a).

6. Conclusion

We demonstrated a silicon strip based heater with integrated diode for optical phase shifting in a silicon photonics platform. The addition of a diode in the heater breaks the voltage symmetry of the device, which can be exploited to allow multiplexed use of its driving pads.

We show the functional benefit of the diodes by demonstrating a PWM based driving scheme which results in a linear correlation between the driving parameter (the duty cycle of the PWM signal) and the induced phase shift. Finally we presented a duobinary solution to operate the circuit, allowing independent control of the elements using the same pair of contact pads.

Funding

European Research Council (ERC) under grant ERC-CoG 725555 PhotonicSWARM.